M. M. Kulyukin, B. Pontecorvo, R. M. Sulyaev, A. I. Filippov, V. M. Tsupko-Sitnikov, and Yu. A. Shcherbakov, Zh. Éksp. Teor. Fiz. 41, 1804 (1962) [Sov. Phys. JETP 14, 1283 (1963)].
[5]S. S. Gershteĭn, Zh. Éksp. Teor. Fiz. 43, 706 (1962) [Sov. Phys. JETP 16, 501 (1963)].
[6]E. Fermi and E. Teller, Phys. Rev. 72, 399 (1947).
[7]V. I. Petrukhin, Yu. D. Prokoshkin, and A. I. Filippov, Yad. Fiz. 6, 1008 (1967) [Sov. J. Nucl. Phys. 6, 734 (1968)].
[8]Studies in Penetration of Charged Particles in Matter, NBS Rep., Washington, 1964.
[9]Yu. G. Budyashov, V. G. Zinov, A. D. Konin, and A. I. Mukhin, Yad. Fiz. 5, 830 (1967) [Sov. J. Nucl. Phys. 5, 589 (1967)].
[10]V. I. Petrukhin, V. E. Risin, I. F. Samënkova, and V. M. Suvorov, JINR Report D1-8876, 1975. Zh. Éksp. Teor. Fiz. 69, 1883 (1975) [Sov. Phys. JETP 42, 955 (1976)].
[11]P. Gombas, Die statistische Theorie des Atoms und ihre Anwendungen, Springer, 1949 (Russ. transl., IIL, 1951).
[12]T. B. Day, G. A. Snow, and T. Sucher, Phys. Rev. Lett. 3, 61 (1959).
[13]M. Leon and H. Bethe, Phys. Rev. 127, 636 (1962). M. Leon, Phys. Lett. 37B, 87 (1971).
[14]S. S. Gershteĭn, V. I. Petrukhin, L. I. Ponomarev, and Yu. D. Prokoshkin, Usp. Fiz. Nauk 97, 3 (1969) [Sov. Phys. Usp. 12, 1 (1969)].
[15]J. Picard *et al.*, Lett. Nuovo Cimento 2, 957 (1971).
[16]W. M. Bugg *et al.*, Phys. Rev. 5D, 2142 (1972).

Translated by C. S. Robinson

Three-reggeon phenomenology in the reaction $p+p\to p+X$

Yu. M. Kazarinov, B. Z. Kopeliovich, L. I. Lapidus, and I. K. Potashnikova

Joint Institute for Nuclear Research
(Submitted September 16, 1975)
Zh. Eksp. Teor. Fiz. 70, 1152–1166 (April 1976)

A statistical analysis has been carried out of data on the reaction $p+p\to p+X$ in the region $|t|<0.6$ $(\text{GeV}/c)^2$ and $x>0.85$. All three-reggeon contributions have been taken into account, including the interference terms. Two sets of parameters have been found which characterize the three-reggeon vertices. In order to explain the deviation of the calculated curves from the experimental energy dependence at low energies and the x dependence for $x<0.85$, a number of diagrams not taken into account in the analysis are proposed. Comparison of the parameter values found with the predictions of the one-pion-exchange model shows good agreement. A discussion is given of a number of processes whose study may provide additional information on the structure of the three-reggeon vertices and the contribution of cuts.

PACS numbers: 12.40.Mm, 12.40.Rr, 13.80.Kp

1. INTRODUCTION

Interest in the experimental and theoretical investigation of the reaction

$$p+p\to p+X \tag{1}$$

at high energies is due to the possibility of carrying out a three-reggeon analysis of the energetic part of the spectra of scattered particles and determining the values of the three-reggeon coupling constants.

The differential cross section for reaction (1) can be related by the unitarity condition to the contribution of three-reggeon diagrams, as shown in Fig. 1, where diagrams with exchange of a pomeron P and reggeons $f=P'$, ω, ρ, and A_2 are summed. In view of the closeness of the trajectories of the second poles, the contributions of the latter are difficult to separate and they are usually replaced by the contribution of an effective pole R.

The expression used in the analysis for the cross section of reaction (1) has the form

$$s\frac{d^2\sigma}{dM^2\,dt}=\sum_{ijk}G_{ijk}(t)\,(1-x)^{\alpha_R(0)-\alpha_i(t)-\alpha_j(t)}\left(\frac{s}{s_0}\right)^{\alpha_R(0)-1}+\left(s\frac{d^2\sigma}{dM^2\,dt}\right)_{nnP}. \tag{2}$$

Here M is the effective mass of the shower produced, t is the square of the 4-momentum transfer, $x=p_L/p_{\max}\approx 1-M^2/s$ (p_L is the longitudinal component of the momentum of the scattered proton, $p_{\max}$ is its maximum value, and s is the square of the total energy of the colliding particles in the c.m.s.). The last term in Eq. (2) corresponds to the contribution of one-pion exchange and is equal to[1]

$$\left(s\frac{d^2\sigma}{dM^2\,dt}\right)_{nnP}=\frac{g^2}{(4\pi)^2}\sigma_{tot}^{\pi N}\frac{(-t)}{(\mu^2-t)^2}\,(1-x)^{1-\alpha_R'\,t}\,e^{Rt}. \tag{3}$$

Here μ is the pion mass, $g^2/4\pi\approx 15$, and $R^2\approx 3.3$ $(\text{GeV}/c)^{-2}$.

The main purpose of the present work is to determine the phenomenological functions $G_{ijk}(t)$ by comparison of Eq. (2) with the experimental data. Preliminary results have been published previously.[2]

Among papers previously published on the questions

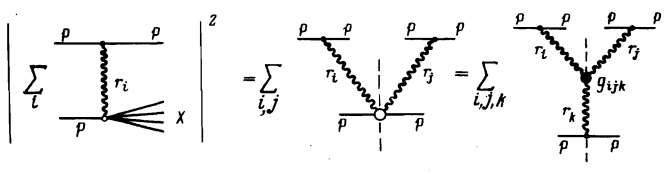

FIG. 1.

being discussed, we must note Refs. 3–5, where the need of taking into account the three-pomeron term in Eq. (2) was demonstrated for the first time, and also Refs. 6 and 7, where the entire set of experimental information on the process (1) was analyzed statistically. However, in the studies published earlier the contribution of interference terms in Eq. (2) was neglected, the analysis procedure contained some weak spots, and the uniqueness of the solutions found was not checked, so that some good solutions were lost. The sum rule for finite masses used in Refs. 6 and 7, which was used to extract information from the low-mass region, cannot be considered a reliable source. As can be seen from our results, the contribution of the *RRR* diagrams is determined with high accuracy from the experimental data in the region of large effective masses, and there is no need to bring in additional information for this purpose.

2. PARAMETRIZATION OF THE FUNCTIONS $G_{ijk}(t)$

For the parameters of the trajectories $\alpha_i(t)=\alpha_i(0)+\alpha_i' t$ in accordance with the data on binary processes we took the values (α' is in units of $(\mathrm{GeV}/c)^{-2}$)

$$\alpha_P(0)=1, \quad \alpha_P'=0.3, \quad \alpha_R(0)=0.5, \quad \alpha_R'=0.75.$$

The contribution of $\pi\pi P$ diagrams was determined[1] on the basis of data on the reaction $p+p\to n+X$.

All the functions $G_{ijk}(t)$ except the interference terms $G_{PRk}(t)$ (see below) are represented in the form

$$G_{iik}(t)=G_{iik}(0)\exp(R_{iik}^2 t), \quad G_{iik}(0)\geqslant 0. \tag{4}$$

The parameters characterizing the interference terms

$$G_{PRk}(t)+G_{RPk}(t)=2\mathrm{Re}\, G_{PRk}(t), \tag{5}$$

cannot be considered free, since they are related by the Bunyakovskiĭ-Schwarz inequality to the values of the parameters in $G_{PPk}(t)$ and $G_{RRk}(t)$.

In order to obtain these limitations, we neglect the contribution of ρ and A_2, since their coupling constants with the nucleon are small.

In the *RPP* interference diagram, which does not contain an s dependence, ω exchange is forbidden. Therefore we can limit ourselves to discussing *fPP* diagrams. Since the complexity of the *fPP* contribution is determined by the signature factors of f and P, the Bunyakovskiĭ-Schwarz inequality reduces to the following:

$$2\mathrm{Re}\, G_{fPP}(t)\leqslant 2\cos\{{}^1/_2\pi[\alpha_P(t)-\alpha_f(t)]\}[G_{ffP}(t)G_{PPP}(t)]^{1/2}. \tag{6}$$

Since $G_{ffP}(t)\leqslant G_{RRP}(t)$, we have

$$\mathrm{Re}\, G_{RPP}(t)\leqslant\cos\{{}^1/_2\pi[\alpha_P(t)-\alpha_R(t)]\}\cdot[G_{RRP}(t)G_{PPP}(t)]^{1/2}. \tag{7}$$

Taking into account (6) and (7), we choose for G_{RPP} the following parametrization:

$$\mathrm{Re}\, G_{RPP}(t)=\sqrt{2}\,\mathrm{Re}\, G_{RPP}(0)\exp(R_{RPP}^2 t)\cos\{{}^1/_2\pi[\alpha_P(t)-\alpha_R(t)]\}. \tag{8}$$

Substituting (8) into (7), we obtain the limitations on the parameter values:

$$2[\mathrm{Re}\, G_{RPP}(0)]^2\leqslant G_{RRP}(0)G_{PPP}(0)\exp[(R_{PPP}^2+R_{RRP}^2-2R_{RPP}^2)t]. \tag{9}$$

The necessity of introducing limitations on the quantity $G_{RPR}(t)$ is not so evident, since R exchange is not dominant in the absorptive parts in Fig. 1. Nevertheless, it can be separated if we utilize the concept of duality and replace integration over the momenta of the created particles in Fig. 1 by summation of the cross sections for resonance production. Then the Bunyakovskiĭ-Schwarz inequality can be written individually for the terms which do not depend on energy.

The contribution of the *PRR* diagrams consists of two parts: *Pff* and *Pωω*. For each of them there exist limitations:

$$2\mathrm{Re}\, G_{Pff}(t)\leqslant 2[G_{fff}(t)G_{PPf}(t)]^{1/2}\cos[{}^1/_2\pi(\alpha_P(t)-\alpha_f(t))] \tag{10}$$

and

$$2\mathrm{Re}\, G_{P\omega\omega}(t)\leqslant 2[G_{\omega\omega f}(t)G_{PPf}(t)]^{1/2}\sin[{}^1/_2\pi(\alpha_P(t)-\alpha_\omega(t))]. \tag{11}$$

The difference in expressions (10) and (11) arose as the result of the difference in the signatures of the ω and f. For the same reason $G_{f\omega\omega}(t)=0$ and $G_{RRR}=G_{fff}+G_{\omega\omega f}$. Having added equations (10) and (11), we obtain

$$\mathrm{Re}\, G_{RPR}(t)\leqslant[G_{RRR}(t)G_{PPR}(t)]^{1/2}. \tag{12}$$

Thus, in contrast to Eq. (9), a convenient parametrization for the quantity G_{PRR} will be

$$\mathrm{Re}\, G_{PRR}(t)=\mathrm{Re}\, G_{PRR}(0)\exp(R_{PRR}^2 t). \tag{13}$$

From Eq. (13) the following condition arises for the parameters of the interference contributions:

$$[\mathrm{Re}\, G_{PRR}(0)]^2\leqslant G_{RRR}(0)G_{PPR}(0)\exp[(R_{PPR}^2+R_{RRR}^2-2R_{PRR}^2)t]. \tag{14}$$

This parametrization corresponds to the variant of strong coupling theory.[8] In weak coupling theory[9] all functions $G_{ijk}(t)$ except $G_{RRk}(t)$ must go to zero as $t\to 0$. We have carried out an analysis of the data on reaction (1) also in this parametrization of the functions $G_{ikj}(t)$. However, the parametrization of $G_{ikj}(t)$ in such a simple form has no deep significance as the result of the strong dependence of $G_{ikj}(t)$ on the contribution of cuts.[10] Therefore in the present work we limit ourselves to discussion of the strong-coupling variants.

3. DATA ANALYSIS PROCEDURE

The statistical analysis of the data was carried out by minimization of the functional

$$\chi^2=\sum_i[\Psi_i-N_k\Psi_i^{\mathrm{theor}}]^2/(\Delta\Psi_i)^2+\sum_k\frac{(N_k-1)^2}{(\Delta N_k)^2}+\sum_j(\Phi_j)^2/(\Delta\Phi_j)^2. \tag{15}$$

Here Ψ_i is the i-th experimental point for the cross section of process (1), Ψ_i^{theor} is its theoretical value given by Eq. (2), $\Delta\Psi_i$ is the experimental error, and N_k is the

TABLE 1. Three-reggeon phenomenology in the reaction $p+p \to p+X$.

s, GeV^2	t, (GeV/c)^2	ΔN, %	N (I)	N (II)
	CERN — Holland — Lancaster — Manchester [11]			
929	$0.24<\|t\|<0.55$	15	0.86±0.03	0.86±0.03
551	$0.15<\|t\|<0.55$	10	0.89±0.03	0.91±0.03
930	$0.35<\|t\|<0.55$	10	1.09±0.03	0.07±0.03
1995	$0.55<\|t\|<0.59$		1	1
	Imperial College — Rutgers [12,13]			
80--480	$\|t\|=0.33$	25	0.98±0.03	0.94±0.03
	$\|t\|=0.45$	25	0.92±0.03	0.88±0.03
108, 213, 285, 503, 752	$0.14<\|t\|<0.18$	15	0.95±0.03	0.96±0.03
	$0.18<\|t\|<0.22$	15	0.95±0.03	0.95±0.03
	$0.22<\|t\|<0.28$	15	0.92±0.03	0.91±0.03
	$0.28<\|t\|<0.38$	15	0.87±0.03	0.85±0.03
	ANL – FNAL [14]			
386	$0.02<\|t\|<0.37$	–	1	1
	Michigan – Rochester [15]			
193	$0.05<\|t\|<0.5$	10	1.05±0.05	1.04±0.04
762	$0.05<\|t\|<0.5$	25	0.86±0.07	0.72±0.07
	Bonn — Hamburg — München [16]			
46.8	$0.05<\|t\|<0.43$	10	1.27±0.04	1.24±0.04
	CERN – Roma [17]			
46.8	$0.1<\|t\|<0.4$	10	1.3±0.04	1.27±0.04
	E. W. Anderson *et al.* [18]			
58.1	$0.16<\|t\|<0.43$	10	0.98±0.03	0.96±0.03

normalization factor which is introduced for the k-th set of experimental points (see Table 1). To assure that the Bunyakovskiĭ-Schwarz inequalities are satisfied in the interference contributions in Eq. (15) we introduced the last term, where

$$\Phi_j=\exp(B\Lambda_j),$$

and the subscript j enumerates the inequalities (9) and (14). The quantity Λ_j, for example for Eq. (9), has the form

$$\Lambda_j=[\operatorname{Re} G_{RPP}(0)]^2-{}^1/_2 G_{RRP}(0)\,G_{PPP}(0)\exp[(R^2_{RRP}+R^2_{PPP}-2R^2_{RPP})t].$$

By choosing a sufficiently large value for the coefficient B we can easily make possible the assumption that with the necessary accuracy

$$\Phi_j\gg 1 \quad \text{for} \quad \Lambda_j>0, \quad \Phi_j\ll 1 \quad \text{for} \quad \Lambda_j<0.$$

Thus, as the result of the last term in Eq. (15), the value of χ^2 rises sharply as soon as inequalities (9) and (14) are violated. The magnitude of the error $\Delta\Phi_j$ is chosen sufficiently large ($\Delta\Phi_j\approx 1$) that the contribution of the last term in Eq. (15) is small in the final solution.

In the analyses of data carried out previously by the χ^2 method, the experimental norms N_k either were fixed or were assumed to be free parameters. In the present work the norms were varied with allowance for the normalization errors in the experimental studies. For this purpose the norms were introduced into the analysis program as free parameters and with each of them we compared an "experimental" point having a nominal value of 1 and an error equal to the experimental error in the normalization.

In Table 1 we have listed the experiments whose results were used in the present analysis and some of their characteristics, including the value of the normalization error used.

TABLE 2. Solution I*.

Parameter	$G_{ijk}(0)$, mb/GeV^2	R^2_{ijk}, (GeV/c)$^{-2}$
G_{PPP}	3.24±0.35	4.25±0.24
G_{RRP}	7.2±1.9	−1.2±0.5
2 Re G_{RPP}	6.9±1.1	8.5±3.7
G_{PPR}	3.2±0.6	1.7±0.4
G_{RRR}	51.9±7.8	0
2 Re G_{PRR}	−9.3±2.2	0

* $\chi^2/\bar{\chi}^2=0.91$.

TABLE 3. Solution II*.

Parameter	$G_{ijk}(0)$, mb/GeV^2	R^2_{ijk}, (GeV/c)$^{-2}$
G_{PPP}	3.23±0.35	4.2±0.3
G_{RRP}	13.2±0.9	0
2 Re G_{RPP}	5.7±4.9	19.5±16.1
G_{PPR}	2±1	1.8±1.1
G_{RRR}	23.6±5.0	0
2 Re G_{PRR}	13.4±4.5	9.7±7.6

* $\chi^2/\bar{\chi}^2=0.93$.

4. RESULTS OF STATISTICAL ANALYSIS

The maximum value of $|t|$ and the minimum value of x for which final results were obtained were determined by analysis of the data with different locations of these limits. The optimum values of $|t|$ and x were chosen so that on decrease of the limit in $|t|$ below $|t|_{max}$ and the limit in x above x_{min} the parameter values did not change within the experimental errors. As a result of this procedure we adopted the values

$$|t|_{max}=0.6 \ (\text{GeV}/c)^2, \quad x_{min}=0.85.$$

The upper limit in x was determined by the energy value at which Regge behavior of the cross sections begins. We chose the value $M^2_{min}=5$ GeV^2. Together with x_{min}, this determined the lower value of s in Table 1.

It should be noted that the leading protons can be the decay product of the $\Delta(1236)$ resonance. Description of such events by means of the RRk diagram has meaning in the spirit of duality. However, the contribution of Δ production reaches a maximum at $x\approx 0.6$ and is negligible in the chosen region $x\geq 0.85$. [19]

In the interval of x and t values indicated above, the data from Table 1 contained 554 experimental points. Of the solutions obtained, we have listed in Tables 2 and 3 two sets of parameter values which permit a statistically satisfactory description to be obtained. We have also given the corresponding values of χ^3. The values of the normalization factors for each solution are given in Table 1.

The quality of description of the experimental data for the reaction $pp \to pX$ by the three-reggeon formula (2) with parameters from solution I is demonstrated graphically in Figs. 2–6.

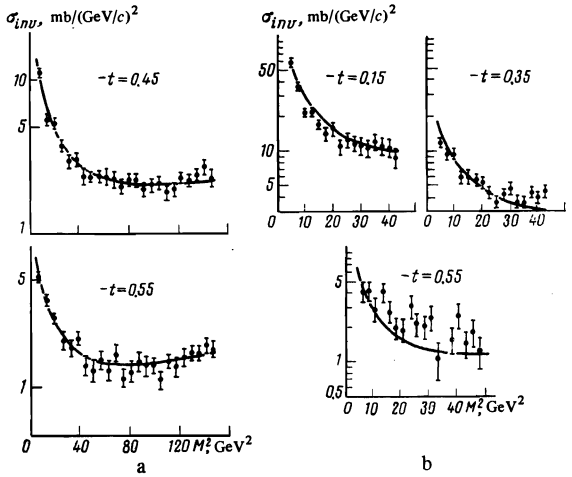

FIG. 2. Data from the CERN-Holland-Lancaster-Manchester Collaboration[11] for the reaction $pp \to pX$: a—for $s = 930$ GeV^2, b—for $s = 551$ GeV^2. The value of t on the curves is given in units of (GeV/c)^2.

In addition to the parameter sets given above, we also found solutions with $\chi^2 \approx \bar{\chi}^2$ but with large values of $G_{RRR}(0) \approx 600$ mb/(GeV/c)^2 and $R^2_{RRR} \approx 30$ (GeV/c)$^{-2}$. From the point of view of evaluation of the three-reggeon vertices, as presented below in Sec. 7, this result is completely in disagreement with the theoretical expectations. Therefore these solutions are not given here.

5. SOME PREDICTIONS

Using the parameter values obtained above, we can make certain predictions and check them by invoking the data of experiments whose results were not used in the analysis.

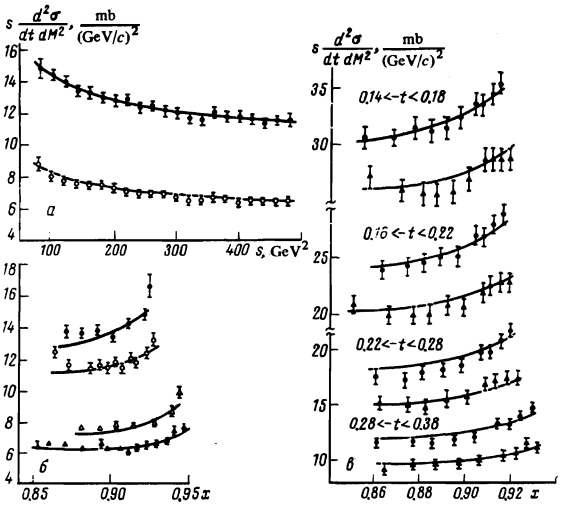

FIG. 3. Data of the Imperial College-Rutgers Collaboration[13,11]: a) ●—$x = 0.82$, $t = -0.33$ (GeV/c)^2; ○—$x = 0.93$, $t = -0.45$ (GeV/c)^2; b) ●—$s = 100$ GeV^2, $t = -0.33$ (GeV/c)^2; ○—$s = 360$ GeV^2, $t = -0.33$ (GeV/c)^2; △—$s = 100$ GeV^2, $t = -0.45$ (GeV/c)^2; ▲—$s = 360$ GeV^2, $t = -0.45$ (GeV/c)^2; c) ●—$s = 108$ GeV, △—$s = 752$ GeV^2 (t on the curves is given in units of (GeV/c)^2).

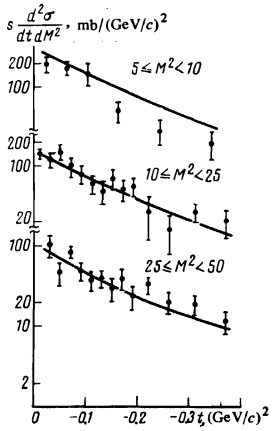

FIG. 4. Data of the ANL-FNAL Collaboration[14]; $s = 386$ GeV^2 (M^2 is given in GeV^2).

The experimental results at $p_{lab} = 69$ GeV/c (Ref. 20) and at $s = 565$ GeV^2 (Ref. 21), which were published very recently, are shown, together with our predictions, in Figs. 7 and 8.

The reaction $p + d \to X + d$ at small t values has been studied by Akimov *et al.*[22] Predictions for this process can be made with certain stipulations. First, in Eq. (2) it is necessary to omit the contributions of the $\pi\pi P$ diagram and also of the ρ and A_2 terms. The latter have a small coupling constant with the nucleon and can be neglected. Then it is necessary to multiply Eq. (2) by the square of the deuteron form factor and by a certain factor; this factor may differ from the square of the ratio of the total cross sections for interaction of pions with deuterons and protons as a result of the fact that the Glauber corrections in the inelastic reaction

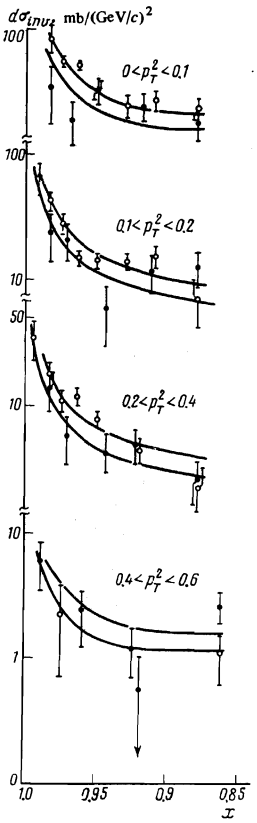

FIG. 5. Data of the Michigan-Rochester Collaboration[15]: ● — $s = 193$ GeV^2, ● —$s = 762$ GeV^2; p_T^2 is given in (GeV/c)^2.

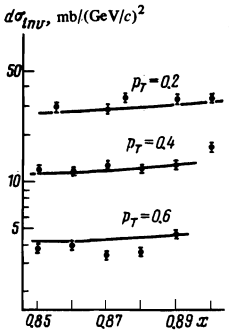

FIG. 6. Data of the Bonn-Hamburg-München Collaboration[16], $s = 46.8$ GeV^2, p_T is in GeV/c. Only the statistical errors are shown.

are given by a different set of diagrams than in the case of elastic scattering. We actually found that this factor is $\approx 20\%$ smaller than $(\sigma_{tot}^{pd}/\sigma_{tot}^{pN})^2$. Thus, the Glauber corrections in the reaction $p+d \to d+X$ are about 10% larger than for elastic scattering. Our predictions, normalized to the data of Ref. 22, are shown in Fig. 9.

6. SOME DIFFICULTIES AND POSSIBLE EXPLANATIONS

A. The main consideration in choice of the limit $x_{min} = 0.85$ is the rapid rise found in Refs. 12 and 13 of the inclusive spectrum on decrease of x below x_{min}. The behavior cannot be described by means of Eq. (2) and evidently is due to other mechanisms. Equation (2) corresponds to the three-reggeon diagrams, i.e., to a model with simple Regge poles. However, it is clear that the $P-P$ and $R-P$ cuts also effectively contribute to Eq. (2). In regard to the $R-R$ cut, its effect is not contained in Eq. (2) as a result of the specific x dependence. The effect of the $R-R$ cut, not reducible to Eq. (2), can explain in principle the behavior discussed above of the spectrum below $x = 0.85$. In order to check this, let us evaluate the contribution of the diagram in Fig. 10.

If for simplicity we replace R by f and use the quasi-eikonal mode, then we can obtain for the contributions of the diagrams of Fig. 10 the expression

$$\Delta\left(s\frac{d^2\sigma}{dM^2\,dt}\right) = \left(s\frac{d^2\sigma}{dM^2\,dt}\right)_{RRP}\frac{2z(z-\lambda+\pi/4)}{[\lambda^2+(\pi/4)^2]}, \qquad (16)$$

where

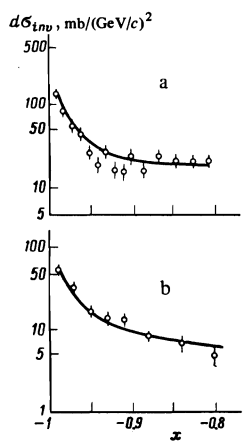

FIG. 7. Comparison of the experimental data[21] at $p_{lab} = 69$ GeV/c and the results of a calculation with the parameters from solution I: a—for $0 < p_T^2 < 0.1$ (GeV/c)^2, b—for $0.1 < p_T^2 < 0.2$ (GeV/c)^2.

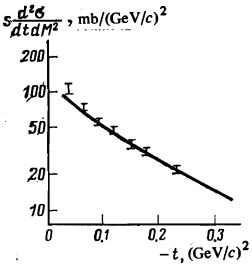

FIG. 8. Comparison of the experimental data[22] at $s = 565$ GeV^2 and $M^2 = 40$ GeV^2 with solution I.

$$z = \frac{C_f\sigma_0}{32\pi}(1-x)^{1/2}e^{-\lambda t/2}, \quad \lambda = R_f^2 - \alpha_R' \ln(1-x).$$

Here it is assumed that f exchange occurs between the protons and one of the fast (in the laboratory system) particles in the shower produced. It was assumed that the coupling constants of f with particles are the same as for the pomeron. Thus, we chose $\sigma_0 \approx 30$ mb and $R_f^2 \approx 1$ (GeV/c)$^{-2}$. The expression $(sd^2\sigma/dM^2dt)_{RRP}$ in the right-hand side of Eq. (16) represents the contribution of the RRP diagram, which is written out in Eq. (2). The quantity C_f is a factor increasing the contribution of the $f-f$ cut as a result of inelasticity in the intermediate states. In Fig. 11 we have shown the x dependence of the quantity $\Delta(sd^2\sigma/dM^2dt)$ for different values of C_f. It is evident that for $C_f \approx 8$ it is possible to describe the experimental data for $x \leq 0.85$.

In comparison with the value of the shower multiplication factor for vacuum branches $C_P \lesssim 2$, the value C_f found above appears surprisingly large. One can, however, give arguments favoring such a difference. If we utilize the idea of duality, the correction to the eikonal as the result of creation in the intermediate state of resonances and showers with low effective mass can be evaluated, carrying out the substitution shown graphically in Fig. 12. If we take into account the contribution of the Pff and fff diagrams to the imaginary part of the amplitude and limit integration over M^2 to the value $M_0^2 = 4$ GeV^2, we obtain

$$C_f \approx \left[1+\left(\frac{3G_{RRP}(0)}{R_{RRP}^2+2\alpha_R'\ln(s/s_0)}+\frac{2G_{RRR}(0)}{R_{RRR}^2+2\alpha_R'\ln(s/s_0)}\right)\times\frac{32\pi[R_f^2+\alpha_R'\ln(s/s_0)]}{s_0^2\sigma_0^2}\right]^2 \underset{s\to\infty}{\approx} \left[1+\frac{16\pi}{\sigma_0^2}(3G_{RRP}+2G_{RRR})\right]^2. \qquad (17)$$

If we now substitute into (17) the parameter values from Table 1, we obtain $C_f \approx 9$. Thus, the evaluation we have carried out has confirmed the possibility of a large contribution of ff branches to the inclusive spectra. From

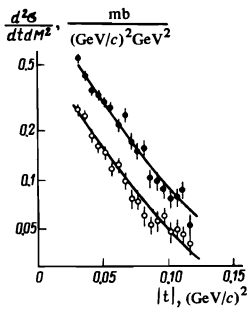

FIG. 9. Comparison of the experimental data for the reaction $p+d \to X+d$ at $p_{lab} = 275$ GeV/c and ● $-M^2 = 11$ GeV^2, ○ $-M^2 = 22$ GeV^2 (Ref. 23) with solution I. See the text for details.

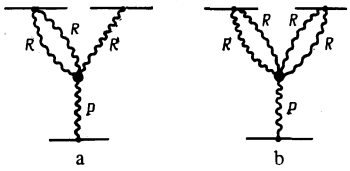

FIG. 10.

Fig. 12 and Eq. (17) it is clear why C_f is large in comparison with C_P. This conclusion is the consequence of a more general result: Diffraction inelastic processes (*PPP* and *PPR*) are suppressed in comparison with the Reggeon contributions (*RRP* and *RRR*). This is evident from Tables 2 and 3 and will be discussed in the next section.

Thus, the $R-R$ cuts cannot be neglected in the region $x \leq 0.85$. At the same time the significant compensation of the contributions of diagrams a and b in Fig. 10 permits us to hope that the effect of $R-R$ cuts for $x \gtrsim 0.85$ is small.

B. As was noted above, the normalization factors for the experiments at comparatively low energy $s \approx 40-60$ GeV^2 differ by about 20% from unity. The casue of this may be the existence of mechanisms which have not been taken into account and which lead to a more rapid dependence on s than given by Eq. (2).[1)]

The observed small departure from an $s^{-1/2}$ dependence may be due to the contribution of the Deck mechanism to the $p+p \to p+N+\pi$ process; the diagram of this process is shown in Fig. 13. The contribution of this diagram to the spectrum in x dies out rapidly with energy as s^{-2}, but at low energies may amount to ~10%.[19]

We note that the diagram shown in Fig. 14 does not contribute to the cross section, since its absorptive parts are reduced for various means of cutoff of the lower reggeons (the amplitude with $\alpha_c(0)=0$ is real).

C. For sufficiently large values of s and M^2 and with increased accuracy of the data a departure from Eq. (2) appears in the energy dependence of the spectra. It is

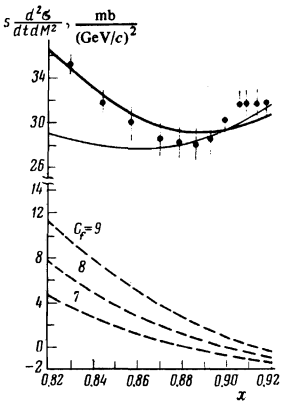

FIG. 11. The data of the Imperial College-Rutgers Collaboration[12] at $s=752$ GeV^2, $|\bar{t}|=0.16$ (GeV/c)^2. The thin solid line is the theoretical value of the cross section according to Eq. (2) with the parameters from solution I. The dashed curves are the result of a calculation with Eq. (16) for different values of C_f. The solid continuous line is the combined cross section for $C_f=8$.

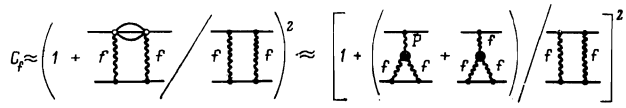

FIG. 12.

natural to expect that the total cross section for interaction of reggeons with nucleons, as occurs also for other hadrons, will begin to increase with energy, which is not taken into account in the pole parametrization (2). However, in the interval of M^2 where the present analysis was carried out and with the accuracy achieved in the experimental data, this effect does not appear.

7. COMPARISON WITH THE ONE-PUIN-EXCHANGE MODEL

Let us compare the parameter values found in Sec. 5 with calculations in the one-pion-exchange (OPE) model. Calculation of the three-reggeon vertices in the OPE model has been carried out in Refs. 24–26. In addition, Boreskov *et al.*[19] utilized a Reggeized OPE model to calculate the cross section for the inclusive reaction (1).

We shall present a simpler derivation than given in Ref. 24 of the expression for the three-reggeon vertices in the OPE model. In this model the diagram in Fig. 1 is converted into the diagram of Fig. 15.

At $t=0$ the following expression for G_{ijk} corresponds to this diagram:

$$G_{ijk}(0)=g_{NNi}g_{NNj}g_{NNk}g_{\pi\pi i}g_{\pi\pi j}g_{\pi\pi k}\eta_i(0)\,\eta_j^*(0)\,I_{ijk}, \tag{18}$$

where g_{NNi} and $g_{\pi\pi i}$ are the coupling constants of reggeon i with the nucleon and pion, $\eta(t)$ is a signature factor, and

$$I_{ijk}=\frac{3}{(4\pi)^4 s_0}\int_{-\infty}^{0}\frac{du}{(\mu^2-u)^2}\left(\frac{\mu^2-u}{s_0}\right)^{\alpha_i+\alpha_j}F(u)\int_0^{-u/(\mu^2-u)}\left(\frac{M_1^2}{M^2}\right)^{\alpha_k^{(0)}}d\left(\frac{M_1^2}{M^2}\right). \tag{19}$$

Here u is the squared four-momentum of the virtual pion, μ is its mass, and M_1 is the energy corresponding to r_k exchange.

Let us explain the structure of expression (19). The factor 3 takes into account the different charge states of the pion, and $(\mu^2-u)^{-2}$ is the square of the virtual-pion propagator.

The energy which is assigned to r_i and r_j exchanges is $(\mu^2+\varkappa_\perp^2)s/(M^2-M_1^2)$, where $\varkappa_\perp$ is the transverse component of the momentum of the created pion. Therefore it follows from comparison with Eq. (2) that the factor

$$[(\mu^2+\varkappa_\perp^2)M^2/s_0(M^2-M_1^2)]^{\alpha_i+\alpha_j}$$

must be included in G_{ijk}. It is easy to show also that

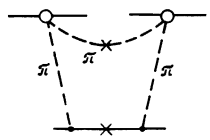

FIG. 13.

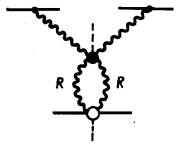

FIG. 14.

$$\mu^2+\varkappa_\perp^2\approx(\mu^2-u)\,(1-M_i^2/M^2). \tag{20}$$

As a result in Eq. (19) there remains the factor $[(\mu^2-u)/s_0]^{\alpha_i+\alpha_j}$.

The form factor $F(u)$ takes into account the departure from the mass shell. It was chosen in the form $F(u)=\exp(R^2u)$, where $R^2\approx 1$ (GeV/c)$^{-2}$. [19]

Since the minimum value of $|u|$ is

$$|u|_{min}=M_i^2\mu^2/(M^2-M_i^2),$$

integration over M_1^2/M^2 in Eq. (2) is bounded by the value $-u/(\mu^2-u)$.

The values of $G_{ijk}(0)$ calculated in accordance with Eqs. (18) and (19) are given below

$$\begin{aligned} &G_{PPP}(0)=4, \quad G_{RRP}(0)=17, \quad 2\,\mathrm{Re}\,G_{RPP}(0)=10.7,\\ &G_{PPR}(0)=5.4, \quad G_{RRR}(0)=27.4, \quad 2\,\mathrm{Re}\,G_{PRR}(0)=15. \end{aligned} \tag{21}$$

In these calculations only the contribution of the f was taken into account, since the ρ and A_2 contributions are suppressed and ω exchange is forbidden in the diagram of Fig. 15. In addition, it was assumed that

$$g_{NNf}g_{\pi\pi f}\approx g_{NNP}g_{\pi\pi P}=s_0\sigma_{tot}^{\pi N}.$$

Comparison of the above values (21) with the results of a statistical analysis of the experimental data on reaction (1) with the aid of Eq. (2) demonstrates good agreement with the parameter values. The fact that $G_{PPk}\ll G_{RRk}$ receives a natural explanation, since for $r_i=r_j=R$ the expression (19) becomes singular as $\mu^2\to 0$.

The dependence of the functions $G_{ijk}(t)$ on t predicted by OPE is steeper than that observed experimentally. This is not too surprising, since the contribution of cuts was not taken into account. For the ω contribution in R it is necessary to take into account, for example, the diagrams shown in Fig. 16. The contribution of diagram a in Fig. 16 is suppressed several times in comparison with the contribution of diagram b. This is explained by the singularity noted above at $\mu^2\to 0$ in expression (20) for the *ffK* diagram. In order to evaluate the role of diagram b in Fig. 16, we will utilize data on the photoproduction of π^0 mesons and vector dominance. Then it is easy to show that

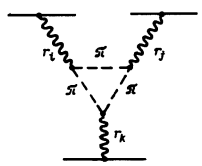

FIG. 15.

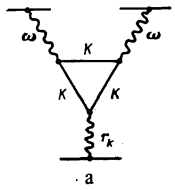

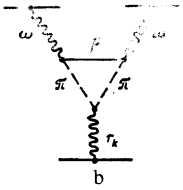

FIG. 16.

$$G_{\omega\omega k}(0)=\frac{3g_{NNk}g_{\pi\pi k}}{16\pi^3(\alpha_k+1)}\,\frac{f_\rho^2}{4\pi\alpha}\,\frac{d\sigma^{\gamma N\to\pi^0 N}(s/M^2)}{dt}\Big|_{t=0}\left(\frac{s}{M^2}\right)^{2-2\alpha_\omega} I_{\omega\omega k}, \tag{22}$$

where

$$I_{\omega\omega k}=\int_{-\infty}^{0} du\,\frac{\exp(R_i^2u)}{(\mu^2-u)^2}\left(\frac{m_\rho^2-u}{s_0}\right)^{2\alpha_\omega}\left(\frac{-u}{m_\rho^2-u}\right)^{1+\alpha_k}. \tag{23}$$

Here f_ρ is the constant of the transition $\gamma\to\rho$ and α is the fine-structure constant. After simple calculations we find from Eqs. (22) and (23) that $G_{\omega\omega k}(0)$ is about an order of magnitude smaller than $G_{ffk}(0)$. Thus, one of the main predictions of OPE is f-dominance among the secondary trajectories (in contrast to the exchange degeneracy in binary processes).

8. WHAT IS INTERESTING TO MEASURE?

Interest is naturally presented by the separation of the contributions of the poles f, ω, ρ, and A_2. Let us consider the energy-independent diagram $G_{RRP}(t)$. We emphasize first of all that the contributions of poles having different quantum numbers do not interfere in this case:

$$G_{RRP}=G_{ffP}+G_{\omega\omega P}+G_{\rho\rho P}+G_{A_1A_2P}. \tag{24}$$

Hence it follows immediately that the vertex G_{RRP} in the reaction with antiprotons $\bar p+p\to\bar p+X$ must be the same as in process (1). The contribution of ω, ρ, and A_2 in Eq. (24) can be found, for example, by studying the energy-independent contributions to the spectra of the reactions

$$\gamma+p\to\pi^0+X, \quad \pi^+(\pi^-)+p\to\pi^0+X \quad \pi^-+p\to\eta^0+X. \tag{25}$$

Special interest is associated with the study of polarization effects in the process (1). The measurement of spin effects is most sensitive to the contribution of branchings in the complex-angular-momentum plane.

Polarization effects in inclusive reactions are different in the beam and target fragmentation regions. If, for example, the target is polarized, then in the beam-fragmentation region there is no asymmetry in the interaction cross section if we take into account only three-reggeon diagrams. [27] Therefore the polarization effects in this case are most sensitive to the contribution of the cuts. In Fig. 17 we have shown the diagrams which contribute to the asymmetry of the process.

We note that diagram a in Fig. 17, and also a number of diagrams with a larger number of rescatterings which are not shown here, lead to an interesting dependence of the asymmetry value on the multiplicity of the particles

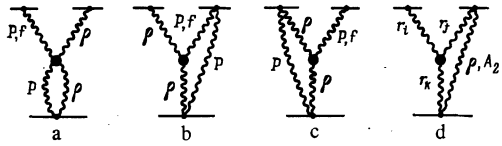

FIG. 17.

produced. If we select events with a number of particles a factor of two greater than the average multiplicity (for a given M^2), then all diagrams contributing to the cross section of the process will lead to asymmetry in the scattering (for example, diagram a, in which both lower reggeons are cut off). Consequently, the asymmetry in the cross section for such events is substantially greater than in a process with normal multiplicity. Thus, the asymmetry should be a rising function of the multiplicity of produced (for fixed M^2).

We shall briefly discuss a number of properties of the dependence of the asymmetry on s, t, and x. We note first of all that since the vacuum branches give a small amplitude with spin flip, it is necessary to have P–R branches, which lead to an energy dependence of the asymmetry proportional[28] to $s^{-1/2}$. It is also known that the main contribution to the amplitude with spin flip is from the reggeons ρ and A_2. However, in contrast to elastic pp scattering, in diagrams a, b, and c of Fig. 17 instead of exchange ρ-A_2 degeneracy we should expect ρ dominance (see Section 7). Therefore the contribution of these diagrams should change sign on the substitution $p \to \bar{p}$. This mirror property will be broken by a small admixture of A_2 contribution and by the contribution of diagram d, where ρ-A_2 degeneracy exists. At the same time on the substitution $p \to n$ of the diagrams in Fig. 17 change their sign. Consequently, the asymmetry in the process $n + p\uparrow \to n + X$ differs in sign from the asymmetry in process (1). We note also that ρ dominance leads to the result that the contribution to the asymmetry of diagrams a and b in Fig. 17 should in the region $x \to 1$ have a behavior of the double-zero type in the region $t = -0.6$ $(\mathrm{GeV}/c)^2$, like the polarization in elastic πP scattering. It is true that a branching contribution strengthened in comparison with elastic scattering can produce a shift of the zero in the residue in the region of small $|t|$ values.

Diagrams c and d in Fig. 17 do not have a double zero. The mirror properties noted above and the presence of a double zero at $t = -0.6$ $(\mathrm{GeV}/c)^2$ occur also for such processes as $\pi^\pm p \to \pi^\pm X$, $K^\pm p \to K^\pm X$.

Let us now discuss the target-fragmentation region. Here polarization effects are possible even without the contribution of branches. In addition, a part of the polarization exists which is independent of energy. However, as noted above, the secondary reggeons do not interfere in the energy-independent part. Therefore in the pole approach the effect is due only to f–P interference and should be small, since f and P lead to a small amplitude with spin flip. The main effect should be expected from the contribution of branches. In this case for $x \to 1$ the energy-independent contribution to the polarization should die out as $(1-x)^{1-2\alpha' k^2 t}$.

9. CONCLUSION

The analysis which we have carried out has shown that three-reggeon phenomenology permits one to obtain a good description of the experimental data on process (1) in the region

$$x \geqslant 0.85, \quad |t| < 0.6 \ (\mathrm{GeV}/c)^2, \ M^2 > 5 \ \mathrm{GeV}^2$$

For the vertex functions a parametrization was used which corresponds directly to the strong-coupling variant. The good qualitative description achieved is not, however, an argument in favor of this variant. With weak coupling the large contribution of the cuts radically changes the t dependence of the vertex functions and simulates the variant of strong pomeron interaction.[10]

In contrast to the previous studies, we have taken into account interference diagrams and carried out the statistical analysis more carefully. As a result we have found several solutions—parameter sets. The predictions obtained on the basis of these solutions are in good agreement with the new data at small t values. Comparison with data on the process $p + d \to d + X$ indicates an appreciable difference in the elastic and inelastic Glauber corrections.

We have discussed additional mechanisms which can lead to appreciable corrections. The Deck diagram leads to a different s dependence; R–R cuts can provide an unusual behavior in the variable x.

The results of calculation of $G_{ijk}(0)$ in the OPE model have been compared with the results of the statistical analysis. Good correspondence of the calculations with the parameter values found has been established. We have noted the set of reactions which must be studied in order to separate the contributions of the various secondary trajectories in the energy-independent part of the three-reggeon functions.

Polarization effects in inclusive processes are discussed with the aim of studying the contributions of cuts. We have pointed out features in the energy dependence, the t dependence, and also the mirror-symmetry property for a number of inclusive processes, which are due to the contribution of two types of cuts.

The authors are grateful to Ya. I. Azkimov, E. M. Levin, L. A. Ponomarev, and V. A. Khoze for helpful discussions.

[1)] In order to avoid this difficulty, Dakhno[23] introduced additional terms with $\alpha_k(0) \leqslant 0$.

[1] M. Bishari, Phys. Lett. B38, 510 (1972); preprint LBL-2066, 1973.
[2] Yu. M. Kazarinov, B. Z. Kopeliovich, L. I. Lapidus, and I. K. Potashnikova, Proc. XVIII Intern. Conf. on High Energy Physics, London, 1974.
[3] A. B. Kaidalov, V. A. Khoze, Y. F. Pirogov, and N. L. Ter-Isaakyan, Phys. Lett. B45, 493 (1973).
[4] A. Capella, Phys. Rev. D8, 2047 (1973).
[5] D. Amati, L. Caneshi, and M. Ciafolini, Nucl. Phys. B62, 173 (1973).
[6] D. P. Roy and R. G. Roberts, Nucl. Phys. B77, 240 (1974).

[7]R. D. Field and G. C. Fox, preprint CALT-68-434, 1974.
[8]A. A. Migdal, A. M. Polyakov, and K. A. Ter-Martirosyan, Zh. Éksp. Teor. Fiz. 67, 848 (1974) [Sov. Phys. JETP 40, 420 (1974)].
[9]V. N. Gribov, Yad. Fiz. 17, 603 (1973) [Sov. J. Nucl. Phys. 17, 313 (1974)].
[10]Ya. I. Azimov, V. A. Khoze, E. M. Levin, and M. G. Ryskin, Nucl. Phys. B89, 508 (1975).
[11]M. G. Albrow *et al.*, Nucl. Phys. B51, 388 (1973); B54, 6 (1973).
[12]K. Abe *et al.*, Phys. Rev. Lett. 31, 1530 (1974).
[13]F. Sannes *et al.*, Phys. Rev. Lett. 30, 766 (1973).
[14]S. J. Barish *et al.*, Phys. Rev. Lett. 31, 1080 (1973).
[15]J. W. Chapman and C. M. Bromberg, preprint UMBC 73-21, 1973.
[16]V. Blobel *et al.*, preprint DESY, 4048/73, 1973.
[17]J. V. Allaby *et al.*, Nucl. Phys. B52, 316 (1973).
[18]E. W. Anderson *et al.*, Phys. Rev. Lett. 19, 198 (1967).
[19]K. G. Boreskov, A. B. Kaidalov, and L. A. Ponomarev, preprint ITEP-43, Moscow, 1973.
[20]Kh. Bialkovska *et al.*, preprint, Institute of High Energy Physics M-11, 1975.
[21]R. Schamberger *et al.*, Phys. Rev. Lett. 34, 1121 (1975).
[22]Yu. K. Akimov *et al.*, Phys. Rev. Lett. 35, 766 (1975).
[23]L. Dakhno, preprint, Institute of High Energy Physics, Division of Theoretical Physics, 75-59, 1975.
[24]H. D. I. Abarbanel, G. F. Chew, M. L. Goldberger, and L. M. Saunders, Ann. Phys. (N. Y.) 73, 156 (1972).
[25]S. C. Sorensen, Phys. Rev. D6, 2554 (1972).
[26]R. Shankar, Nucl. Phys. B79, 126 (1974).
[27]H. D. I. Abarbanel and D. J. Gross, Phys. Rev. Lett. 26, 732 (1971).
[28]R. D. Field, Proc. of Summer Studies on High Energy Physics with Polarized Beams, ANL/HEP 75-02, 1975.

Translated by C. S. Robinson

Direct measurement of the rates of formation of the molecules $pp\mu$ and $pd\mu$ in gaseous hydrogen

V. M. Bystritskiĭ, V. P. Dzhelepov, V. I. Petrukhin, A. I. Rudenko, V. M. Suvorov, V. V. Fil'chenkov, G. Chemnitz, N. N. Khovanskiĭ, and V. A. Khomenko

Joint Institute for Nuclear Research
(Submitted November 18, 1975)
Zh. Eksp. Teor. Fiz. **70**, 1167–1177 (April 1976)

A gas target filled with H_2, H_2+Xe, and H_2+Xe+D_2 (xenon concentration 3×10^{-5}, deuterium $\approx7\%$) at a pressure of 40 atm in the muon beam of the JINR synchrocyclotron has been used to measure the rate of formation of the mesic molecules $pp\mu$ and $pd\mu$, and also the ratio of the rates of transfer of the muon from the proton and deuteron to xenon. The following results were obtained:
$\lambda_{pp\mu}=(2.34\pm0.17)\cdot10^6$ sec^{-1},
$\lambda_{pd\mu}=(5.53\pm0.16)\cdot10^6$ sec^{-1},
$B=1.62\pm0.05$.

PACS numbers: 36.10.Dr

With the coming into operation of high-current accelerators—meson factories—we have a real possibility of accomplishing such fundamentally important experiments as precision measurements of the rate of μ capture in gaseous hydrogen and deuterium. For choice of the optimal conditions and correct interpretation of the data of these experiments, it is necessary to know the parameters of the mesic-atom processes occurring in hydrogen—formation of $pp\mu$ and $pd\mu$ molecules. It is important to emphasize that the determination of these parameters must be carried out specifically in gaseous hydrogen, in view of the possible nontrivial dependence on the density of hydrogen.

The experimental and theoretical values of the rates of formation of the mesic molecules $pp\mu$ ($\lambda_{pp\mu}$) and $pd\mu$ ($\lambda_{pd\mu}$) are given in Table 1. Until recently no direct measurements of $\lambda_{pd\mu}$ had been made in a gas. In earlier work by some of the present authors[10] an attempt was made to evaluate $\lambda_{pd\mu}$ on the basis of the measured yield of muons from the catalysis reaction (1a) in the $pd\mu$ molecule

$$p d\mu \begin{cases} \nearrow \mathrm{He}^3+\mu^-+5.3\ \mathrm{MeV} & \text{(1a)} \\ \searrow \mathrm{He}^3\mu+\gamma+5.5\ \mathrm{MeV} & \text{(1b)} \end{cases},$$

it being necessary for this purpose to utilize various data on reactions (1a) and (1b) obtained in experiments with liquid hydrogen. In our recent work[6] the value of $\lambda_{pd\mu}$ in a gas was found by analysis of the time distribution of the γ rays from reaction (1b) with use of the value obtained by Bleser *et al.*[1] for the rate of reaction (1b) and with the assumption of a statistical nature of the population of the spin states of the $d\mu$ system. The purpose of the present work was direct measurement of $\lambda_{pp\mu}$ and $\lambda_{pd\mu}$ in gaseous hydrogen. In the course of the work we also obtained the ratio B of the muon transfer rates from the proton and deuteron to xenon.

METHOD OF MEASUREMENT

The work utilized a method similar to that described elsewhere[2,4] and based on use of a mixture of hydro-